J. Biophotonics **6**, No. 11–12, 911–919 (2013) / **DOI** 10.1002/jbio.201200103

Journal of BIOPHOTONICS

FULL ARTICLE

Applications of ultrasensitive wavelength-modulated differential photothermal radiometry to noninvasive glucose detection in blood serum

Xinxin Guo[*,1], *Andreas Mandelis*[1], *and Bernard Zinman*[2]

[1] Center for Advanced Diffusion-Wave Technologies (CADIFT), Department of Mechanical and Industrial Engineering, University of Toronto, ON M5S 3G8, Canada
[2] Mount Sinai Hospital, Samuel Lunenfeld Research Institute, University of Toronto, Toronto, ON M5T 3L9, Canada

Received 29 May 2012, revised 1 August 2012, accepted 8 August 2012
Published online 28 August 2012

Key words: biosensor, glucose, serum, MIR, wavelength-modulated differential photothermal radiometry

Wavelength-Modulated Differential Laser Photothermal Radiometry (WM-DPTR) has been designed for noninvasive glucose measurements in the mid-infrared (MIR) range. Glucose measurements in human blood serum in the physiological range (20–320 mg/dl) with predicted error <10.3 mg/dl demonstrated high sensitivity and accuracy to meet wide clinical detection requirements, ranging from hypoglycemia to hyperglycemia. The glucose sensitivity and specificity of WM-DPTR stem from the subtraction of the simultaneously measured signals from two excitation laser beams at wavelengths near the peak and the baseline of the strongest interference-free glucose absorption band in the MIR range. It was found that the serum glucose sensitivity and measurement precision strongly depend on the tunability and stability of the intensity ratio and the phase shift of the two laser beams. This level of accuracy was favorably compared to other MIR techniques. WM-DPTR has shown excellent potential to be developed into a clinically viable noninvasive glucose biosensor.

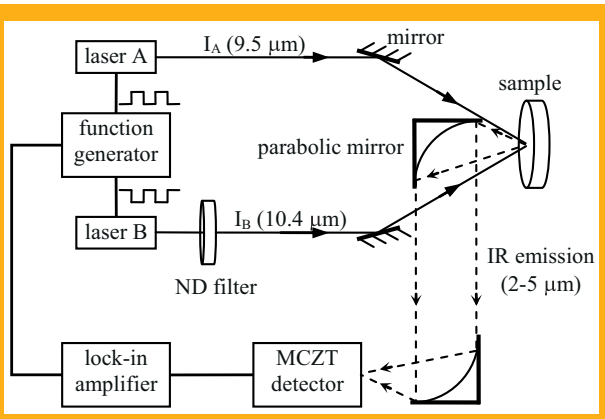

WM-DPTR system setup for glucose measurement.

1. Introduction

Diabetes is very prevalent in today's world. According to the latest WHO diabetes fact sheet (2011), it has affected the lives of 346 million people world wide. The great impact of diabetes on human health is the potential damage to heart, blood vessels, eyes, kidneys and nerves over time. It is estimated that the death overall risk among people with diabetes is at least two times higher than for people without diabetes. Blood glucose (BG) monitoring has been established as a valuable tool in the management of diabetes. Self monitoring of blood glucose (SMBG) is a fundamental tool for the proper adjustment of diabetes treatment. In the newly published Guidelines and Recommendations for Laboratory Analysis in the Diagnosis and Management of Diabetes Mellitus [1, 2], SMBG is recommended for all insulin-

* Corresponding author: e-mail: guox@mie.utoronto.ca, Phone: +1 416 978 1287

treated patients with diabetes. The current approaches recommended by the American Diabetes Association to home glucose monitoring, non-continuous [3] and continuous [4], are invasive or minimally invasive. Non-continuous glucose monitoring involves pricking a fingertip to obtain a blood sample and using a glucose meter to measure the glucose level in the sample. Continuous glucose monitoring (CGM) systems use a tiny sensor inserted under the skin to check glucose levels in the tissue fluid. A transmitter sends glucose measurement data to a wireless monitor. Current CGM devices are not as accurate and reliable as BG meters and sensor lifetimes are only 3–7 days. Researchers are working on longer lifetime and more precise sensors, like the long duration implantable sensor [5], the tattoo-like glucose sensor [6, 7] and a glucose-detection-in-tear device [8, 9]. However the present accurate finger-prickle methodology is not well tolerated by patients because it is painful and expensive. Despite recommendations for frequent home BG monitoring (at least 3 times a day), it was estimated that at least 36% of all patients treated with insulin checked their BG less than once per day in 2006 [2]. Numerous investigators have been attracted to the idea of using a noninvasive device for determining blood glucose which would permit more frequent testing and a tighter control of diabetes. Since 2000, more than 18,200 research articles have been published (an average of 1,485 articles per year) and more than 3,430 US patents have been granted (an average 280 patents per year) for noninvasive glucose monitoring (NGM) devices and methods. Nevertheless, despite some encouraging results and great efforts made over the past years, there is still no NGM device available at present for use in clinical practice [1, 2].

Among all the noninvasive glucose monitoring attempts, optical methods are the most promising ones, passing a selected beam of light into the human body and then determining the level of glucose from an analysis of the resulting spectrum [10–16]. This approach is truly noninvasive, in that there is no need to collect a sample of blood or interstitial fluid. It also has the potential for continuous glycemic measurements while avoiding the complications associated with implantable glucose biosensor technologies. However, noninvasive blood glucose monitoring represents a great challenge and involves full understanding of the chemistry, physics, physiology, and optics associated with the measurement. Only optical techniques with high degree of glucose selectivity and sensitivity can be successful.

In the past two decades, active research areas have included polarimetry [17, 18], Raman spectroscopy [19, 20], diffuse reflection spectroscopy [21, 22], absorption/transmission spectroscopy [23, 24], thermal emission spectroscopy [25, 26], fluorescence spectroscopy [27, 28] and photoacoustic spectroscopy [29–31]. The spectral range of highest interest has been the near infrared (NIR) because of the relatively low water absorption and hence the deeper penetration into blood vessels [10, 12, 13]. However, the weak glucose absorption bands (overtone and combination bands) and confounding bands from other blood constituents have strongly hampered the feasibility of NIR methods. For this reason NIR spectroscopy is purely empirical and not particularly suited for qualitative work. However, using multivariate statistical techniques on the NIR spectrum does allow for quantitative analysis [11], which is still a challenge.

In contrast, the MIR region involves a prominent glucose absorption band which is peaked at ca. 9.7 μm [32], and is isolated from other interfering peaks in human blood [26, 30, 31, 33–35]. The peak absorption is ∼ three orders higher than that in the NIR region [10]. Difficulties in the MIR range are the strong water absorption and the resulting background fluctuation for single-ended and contact methods. The absorption method [34, 35] is limited by the small optical path (25 μm). Photoacoustic methods [29, 31, 33] and the thermal radiation method [25, 26], are suffering from water baseline variation (water accumulation) due to the intrinsically contacting nature of the techniques.

Recently we developed a noninvasive and non-contacting technique, wavelength modulated differential laser photothermal radiometry (WM-DPTR) for continuous or intermittent glucose monitoring in the MIR range [36–39]. The WM-DPTR method consists of out-of-phase modulated laser-beam excitation at two discrete wavelengths near the peak (∼9.5 μm) and the baseline (∼10.4 μm) of the aforementioned glucose absorption band. Two quantum cascade lasers (QCL) are used, resulting in a differential blackbody emission detected via a HgCdZnTe (MCZT) detector (2–5 μm spectral detection bandwidth) as a photothermal energy up-conversion process. The differential method suppresses the strong background signal due to water absorption while the narrow detector spectral bandwidth eliminates source-detector interference, thus greatly enhancing glucose detection sensitivity. The non-contact and back-scattered detection features make WM-DPTR feasible for clinical applications. As a MIR method which can not reach deep blood vessels, WM-DPTR is intended to measure glucose concentration within the interstitial fluid (ISF), which is similar to that in blood with only approx. a 10-minute time delay [40]. We have demonstrated the high glucose sensitivity of WM-DPRT in water-glucose mixture measurements in the physiological concentration range [37, 39]. In this paper the application of WM-DPTR will be further extended to more biologically rele-

vant mixtures of human serum and glucose, which is an appropriate substitute for the interstitial fluid [41].

2. Method and materials

2.1 Theory

The photothermal radiometric signal generation process involves conversion of absorbed optical energy into thermal energy emitted in the infrared range. In WM-DPTR a differential photothermal radiometric signal is generated from sequential optical absorption of two out-of-phase square-wave modulated laser beams by a semi-infinite medium [39]. The sensitive glucose detection arises from the selective absorption of the glucose molecule at two excitation wavelengths (peak and baseline of the MIR glucose absorption band). The photothermal radiometry (PTR) signal generated by a single laser in the one-dimensional limit is given as follows:

$$S_j(t) = \Delta Q_j(t) = \left[\frac{\bar{\mu}_{\mathrm{IR}} K(\lambda_1,\lambda_2)\,\alpha}{2k}\right] I_{0j}\mu_{ej}\tau_{tj} \times \left\{ \begin{array}{l} \dfrac{1}{\bar{\mu}_{\mathrm{IR}}+\mu_{ej}}\left[W\left(\sqrt{\dfrac{t}{\tau_{tj}}}\right)+W\left(\sqrt{\dfrac{t}{\tau_{\mathrm{IR}}}}\right)-2\right] \\ +\dfrac{1}{\bar{\mu}_{\mathrm{IR}}-\mu_{ej}}\left[W\left(\sqrt{\dfrac{t}{\tau_{tj}}}\right)-W\left(\sqrt{\dfrac{t}{\tau_{\mathrm{IR}}}}\right)\right] \\ +\dfrac{2}{\bar{\mu}_{\mathrm{IR}}}\left\{2\sqrt{\dfrac{t}{\pi\tau_{tj}}}-\sqrt{\dfrac{\tau_{\mathrm{IR}}}{\tau_{tj}}}\left[1-W\left(\sqrt{\dfrac{t}{\tau_{\mathrm{IR}}}}\right)\right]\right\} \end{array} \right\}; \quad j = A, B \tag{1}$$

where $\bar{\mu}_{\mathrm{IR}}$ is the spectrally-weighted IR absorption/emission coefficient for homogeneous absorbers, $K(\lambda_1,\lambda_2)$ is a factor related to the detector spectral collection bandwidth $[\lambda_1,\lambda_2]$, α and k are thermal diffusivity and thermal conductivity of the medium, respectively, I_{0j} is laser beam intensity, μ_{ej} is optical absorption coefficient, $\tau_{tj} \equiv \dfrac{1}{\mu_{ej}^2\alpha}$ is a photothermal time constant indicating heat conduction in the photo-excited medium from a subsurface distance equal to the optical absorption depth, $W(x) \equiv \mathrm{e}^{x^2}\,\mathrm{erfc}\,(x)$, and $\tau_{\mathrm{IR}} \equiv \dfrac{1}{\alpha\bar{\mu}_{\mathrm{IR}}^2}$, a photothermal time constant indicating conductive heat transfer from a depth equal to the mean infrared optical absorption/emission depth, $1/\bar{\mu}_{\mathrm{IR}}$.

Over the full square optical waveform repetition period $0 \le t \le \tau_0$, the sequence of photothermal responses is as follows:

$$S_{\mathrm{AB}}(t) = \left\{ \begin{array}{l} \Delta Q_{\mathrm{A}}(t); \quad 0 \le t \le \dfrac{\tau_0}{2} \quad \text{(laser A on; laser B off)} \\ \Delta Q_{\mathrm{A}}(t) - \Delta Q_{\mathrm{A}}\left(t-\dfrac{\tau_0}{2}\right) + \Delta Q_{\mathrm{B}}\left(t-\dfrac{\tau_0}{2}\right); \\ \dfrac{\tau_0}{2} \le t \le \tau_0 \text{ (laser A off; laser B on)} \end{array} \right. \tag{2}$$

With lock-in detection, the final demodulated WM-DPTR signal at the fundamental angular frequency $\omega_0 = 2\pi/\tau_0$ is expressed by amplitude A and phase P:

$$A_{\mathrm{AB}} = \sqrt{\Delta S_{\mathrm{IP}}^2 + \Delta S_Q^2}$$
$$P_{\mathrm{AB}} = \tan^{-1}\left(\frac{\Delta S_Q}{\Delta S_{\mathrm{IP}}}\right) \tag{3}$$

where $\Delta S_{\mathrm{IP}}(\omega_0) = \dfrac{2}{\pi}\,b_1(\omega_0)$ is the in-phase component and $\Delta S_Q(\omega_0) = -\dfrac{2}{\pi}\,a_1(\omega_0)$ is the quadrature with

$$\begin{bmatrix} a_1(\omega_0) \\ b_1(\omega_0) \end{bmatrix} = \frac{\omega_0}{\pi}\int_0^{\tau_0} S_{\mathrm{AB}}(t)\begin{bmatrix} \cos(\omega_0 t) \\ \sin(\omega_0 t) \end{bmatrix} \mathrm{d}t \tag{4}$$

2.2 Experimental setup

Figure 1 shows a diagram of the developed experimental WM-DPTR system. The system consists of two quantum cascade lasers (QCL, 1101-95/104-CW-100-AC, Pranalytica, CA) emitting at 9.5 μm and 10.4 μm, a HgCdZnTe detector (MCZT, PVI-4TE-5, Vigo System, Poland) sensitive in the 2–5 μm spectral bandwidth, a function generator (33220A, Agilent Technologies, CA) generating two phase-locked square waves to modulate the laser beams, and a lock-in amplifier (SR850, Stanford Research Systems, CA). When the two out-of-phase square-wave-modulated laser beams irradiate the sample, a differential PTR signal is generated. The signal is collected by the MCZT detector and then sent to the lock-in amplifier for demodulation through a pair of parobolic mirrors. The intensity ratio of the two lasers is controlled by a motorized variable circular neutral density filter (Reynard Corp, CA) placed in front of laser B and the phase shift between the two laser beams is sensitively controlled by the phase-locked function generator. Both laser output powers are ca. 35 mW with beam sizes ~2.5 mm. To simu-

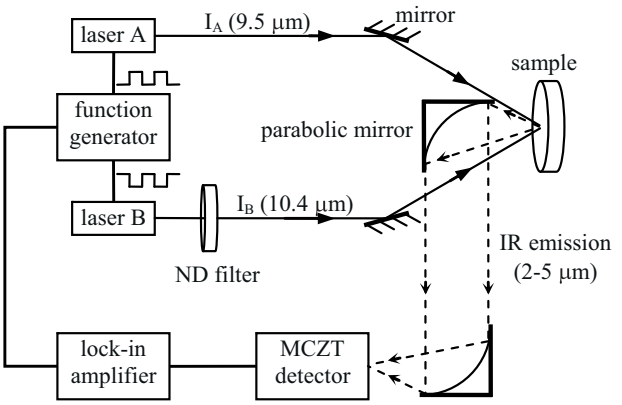

Figure 1 WM-DPTR system setup for glucose measurement. Square-wave modulated radiation from laser A (9.5 μm) and laser B (10.4 μm) co-incident on the sample generate superposed IR emissions. The differential infrared photon flux is collected by the MCZT detector acting as a band pass filter (2–5 μm, dashed line) and sent to a lock-in amplifier. The function generator controls the phase shift between the two laser beams, and the variable circular neutral density (ND) filter controls the intensity ratio of the two lasers I_A/I_B.

late glucose detection in ISF, the laser modulation frequency which controls the WM-DPTR probing depth was set at 150 Hz in order to generate a probe depth ~40 μm in the epidermis layer (~60% water) below the 10–20 μm thick stratum corneum (~10% water) [29].

2.3 Materials

In order to test the feasibility of WM-DPTR for glucose detection in ISF in a clinical context, measurements of human serum were performed with glucose concentrations 20–320 mg/dl, covering the entire hypoglycemic (20–70 mg/dl), euglycemic (70–180 mg/d) and hyperglycemic (180–320 mg/dl) range [42]. Serum-glucose mixtures were obtained by dissolving D-glucose in glucose-depleted base human serum (1016011, American Bilogical Technologies Inc. TX). Glucose concentrations of the mixtures were determined accurately using a biochemistry analyzer (YSI 2700S, Life Sciences, OH). The biochemistry analyzer measurement showed that the base serum contained ~20 mg/dl residual glucose. The sample was contained in a cylindrical cell (R-10-22, International Crystal Laboratories, NJ) with AR-coated ZnSe window on both sides, allowing high transmission of laser beams and IR emissions.

3. Results and discussion

Before the WM-DPTR serum-glucose measurements, FTIR absorption measurements on serum-glucose solution and water-glucose solution were performed to verify that there were no confounding peaks from serum constituents in the MIR range where WM-DPTR operates. Figure 2 shows the FTIR absorption spectra of serum-glucose solution and water-glucose solution in the 8–11 μm wavelength range, coincident with the prominent glucose absorption band. The glucose concentration in both solutions was ~20,000 mg/dl. It can be seen that the serum-glucose spectrum almost overlaps the water-glucose spectrum, which is indicative that no interfering absorptions occur in this region from other serum constituents. The small offset of the two spectra could be due to error in glucose concentration measurements.

Figure 3 displays the distribution of WM-DPTR signals (amplitude A_{AB} and phase P_{AB}) as a function of amplitude ratio R, defined as the ratio of serum PTR amplitudes generated from laser A and laser B alone, $R = A_{AS}/A_{BS}$. It also shows how the WM-DPTR signal distribution changes with glucose concentration from 20 mg/dl to 285 mg/dl. The small error bars of the data points are not shown here for clarity of the trends. The tuning range of amplitude ratio R (0.97–1.02) was controlled with the circular variable ND filter in front of laser B. The phase shift dP, defined as the phase difference between the pure serum signals $dP = P_{AS} - P_{BS}$, was set at 180° by adjusting the waveform modulation phase of laser B relative to that of laser A through the phase-locked function generator. Similarly to our previous water-glucose measurements [37, 39], the amplitude of pure serum, Figure 3(a), forms a V-curve with mini-

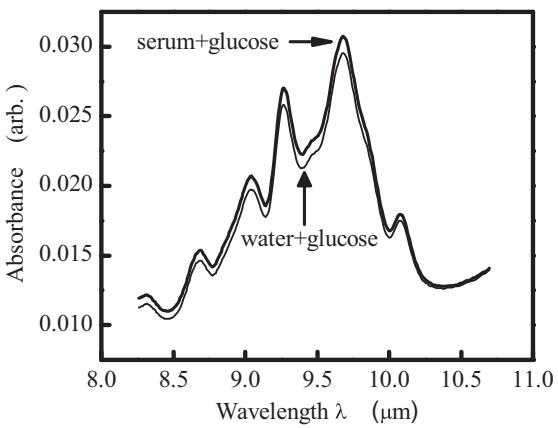

Figure 2 FTIR absorption spectra of serum-glucose solution and water-glucose solution with glucose concentration of 20,000 mg/dl in the mid-infrared range. Water background was not subtracted.

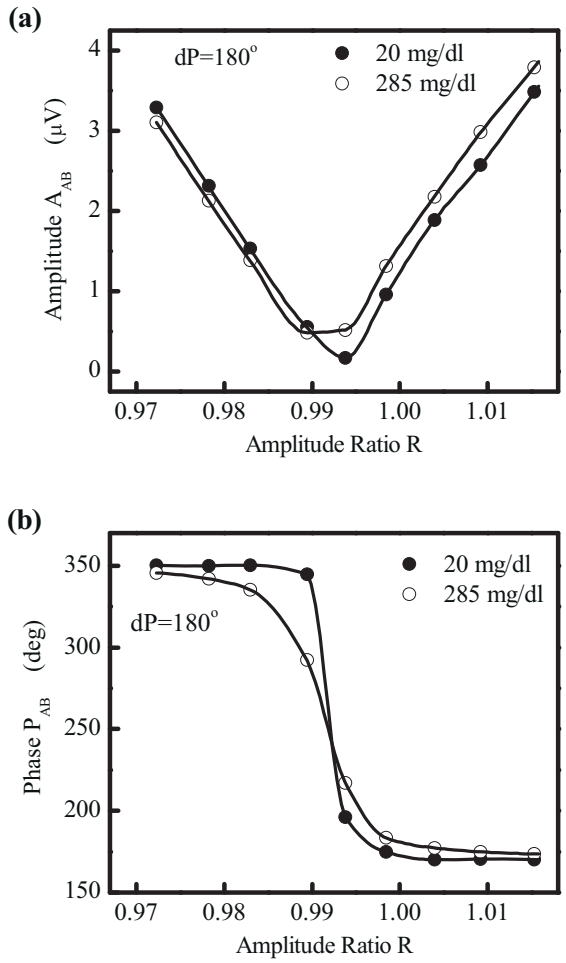

Figure 3 WM-DPTR signal profile of serum-glucose solutions as a function of amplitude ratio R with phase shift $dP = 180°$ and glucose concentration $C_g = 20$ mg/dl and 285 mg/dl. (**a**) amplitude; (**b**) phase. The symbols are experimental data and the lines are interpolated data.

mum close to $R = 1$. When glucose concentration increases from 20 mg/dl to 285 mg/dl, the V-curve rises and shifts toward lower R values. A complicated and asymmetric glucose sensitivity profile is observed: signal rises in the $R > 1$ region and falls in the $R < 1$ region; there is no signal change at $R \sim 0.99$ where the two curves cross. In general, the amplitude is more sensitive to glucose for $R > 1$. The phase of pure serum, Figure 3(b), also shows a similarity to water-glucose measurements. The differential phase of pure serum changes sharply from a value close to P_{BS} to a value close to P_{AS} with amplitude ratio R increasing from 0.97 to 1.02. When glucose concentration increases, the phase transition becomes more gradual. Unlike the amplitude, the complicated and asymmetric phase glucose sensitivity profile displays higher sensitivity in the $R < 1$ region, again, with signal falling for $R < 1$ and rising for $R > 1$. The glucose-insensitive ratio for the phase is around $R = 0.995$.

It was found that glucose sensitivity of WM-DPTR signals is not only affected by the amplitude ratio R as shown in Figure 3, but also by the phase shift dP. Figure 4 exhibits the phase shift influence on glucose sensitivity distribution with phase shift dP deviating $\pm 0.5°$ away from 180°. Figure 4(a) shows the relative amplitude change $\Delta A_{AB}/A_{ABS}$ as a function of amplitude ratio R with phase shift $dP = 180°$, 180.5° and 179.5°. A_{ABS} is the differential amplitude of pure serum and ΔA_{AB} $(= A_{AB} - A_{ABS})$ is the change of the differential amplitude when glucose concentration increases from 20 mg/dl to 285 mg/dl. Amplitude glucose sensitivity exhibits a very narrow and sharp peak around $R \sim 1$ at $dP = 180°$. When phase shift departs from 180° to 180.5° and 179.5°, the peak sensitivity drops greatly, from 2 to ~0.4 with peak position moving toward smaller ($dP = 180.5°$) and larger ($dP = 179.5°$) R values. Figure 4(b) displays absolute differential phase change under the same conditions as Figure 4(a). The phase shift also has a large effect on the narrow phase sensitivity peak near $R \sim 1$, dropping from ~53° to ~17° when dP varies from 180° to either 180.5° or 179.5°. Figure 4 indicates that both WM-DPTR amplitude and phase are sensitive to glucose in serum in a complementary manner, but the amplitude ratio exhibits the largest sensitivity when phase shift $dP = 180°$ which, however, is accompanied by a large measurement error due to the small absolute values of the differential signal and is thus a great challenge to instrumentation control. However, strong R-dependence of glucose sensitivity can still be obtained with phase shift dP set slightly away from 180°, at the cost of some sensitivity. It should be noted that WM-DPTR is an inherently non-linear differential-signal methodology and linearity of signal is also R and dP dependent, as shown in our previous water-glucose study [37, 39]. For clinical applications, an optimized combination of R and dP should be used to achieve three necessary conditions: glucose sensitivity, measurement precision and signal linearity.

Figure 5 presents blood serum glucose measurement results with optimal R-dP combinations 1.004–179.56° for amplitude, Figure 5(a), and 0.988–179.56° for phase, Figure 5(b). The glucose concentration ranges from 20 mg/dl to 320 mg/d with ~40 mg/dl interval. The error bars on data points are from five measurements. Both amplitude and phase responses are essentially linear in glucose concentration in the physiological glucose concentration range (linearity of 0.98 R^2 and 0.99 R^2, respectively), with ~67% total change in amplitude and ~40° total change in phase. "The glucose measurement error, an indicator of glucose sensitivity and measurement repeatability, can be predicted from the deviation of

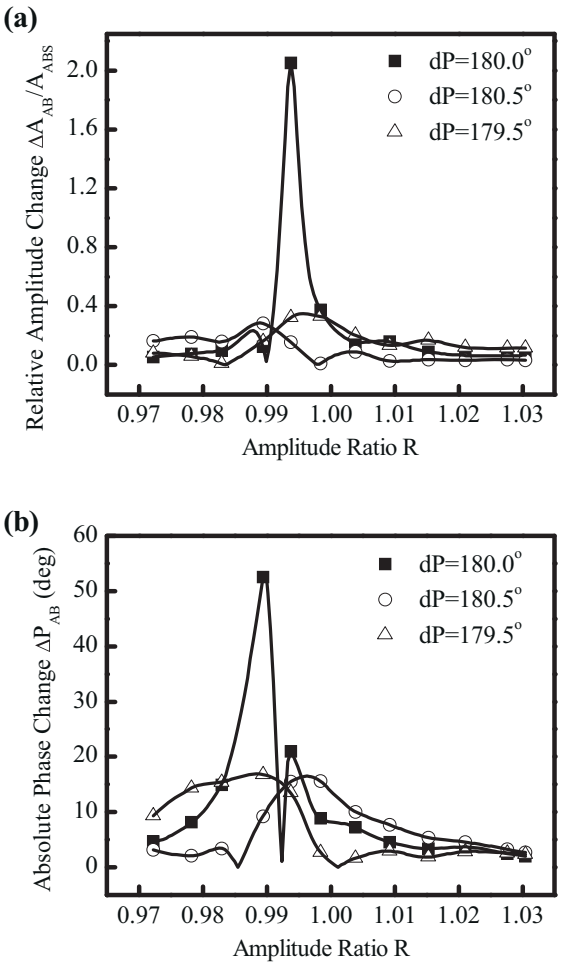

Figure 4 Amplitude ratio R and phase shift dP dependence of WM-DPTR glucose sensitivity. The differential signal changes are due to the 20–285 mg/dl glucose concentration change. (**a**) amplitude; (**b**) phase. The symbols are experimental data and the lines are interpolated data.

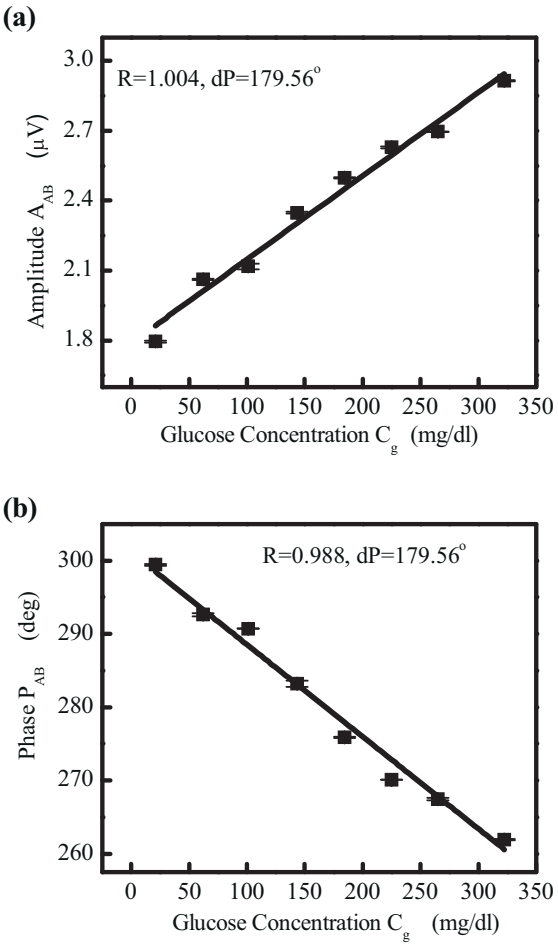

Figure 5 Optimal R – dP combinations for linear WM-DPTR signal response to glucose in serum across the entire physiological glucose concentration range from 20 mg/dl to 320 mg/dl. (**a**) amplitude response; (**b**) phase response.

measurements (data points) from the (best fit) calibration curve using the standard deviation of fitting parameter intercept and slope." The predictive standard error of mean is: 9.2 mg/dl (amplitude) and 6.8 mg/dl (phase) for glucose concentration <75 mg/dl; 14.1 mg/dl (amplitude) and 10.2 mg/dl (phase) for glucose concentration >75 mg/dl. Another pair of R-dP combinations (0.982–179.95° for amplitude and 1.017–179.95° for phase) was also used to measure serum glucose in the hypoglycemic range, as shown in Figure 6. The glucose concentration varies from 20 mg/dl to 80 mg/dl with ~20 mg/dl interval. The amplitude linearly (0.92 R^2) decreases 20% and the phase linearly (0.85 R^2) increases 4° over the low glucose concentration range. The predictive standard error of mean is 12.1 mg/dl for amplitude and 16.1 mg/dl for phase. It is clear from Figure 5 and 6 that different R-dP combinations result in different predictive errors in the hypoglycemic range. Nevertheless, the predictive errors in the above measurements are well below the evaluation criteria for a SMBG device set by the International Organization for Standardization (15 mg/dl for values <75 mg/dl and 20% for values >75 mg/dl) [43], and clinically relevant Clarke-EGA (<70 mg/dl for values <70 mg/dl and 20% for value >70 mg/dl) [44]. There are some other promising techniques operating in the same MIR range. The photoacoustic technique with pulsed light at wavelength 9.68 μm or with modulated light at wavelength 9.67 μm has shown good correlation with blood sugar levels [31] and has demonstrated the feasibility of glucose detection from ISF in epidermis [29]. Thermal emission spectroscopy [25] measured the naturally emitted infrared signals generated from the tympanic membrane in the ear due to changes in glucose concentration in the wavelengths 8.5 μm and 9.6 μm, and has demon-

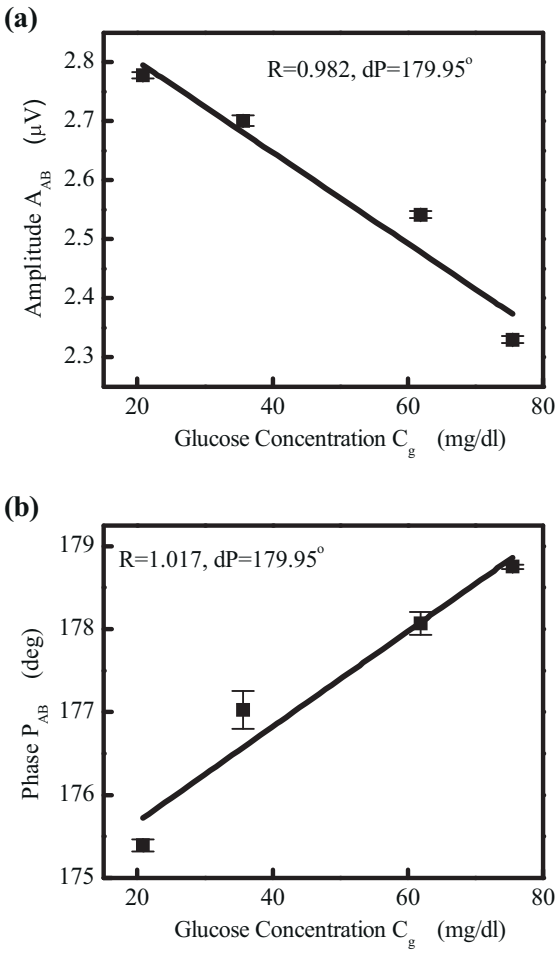

Figure 6 Optimal *R*-d*P* combinations for linear WM-DPTR signal response to glucose in the low glucose concentration range from 20 mg/dl to 80 mg/dl. (**a**) amplitude; (**b**) phase.

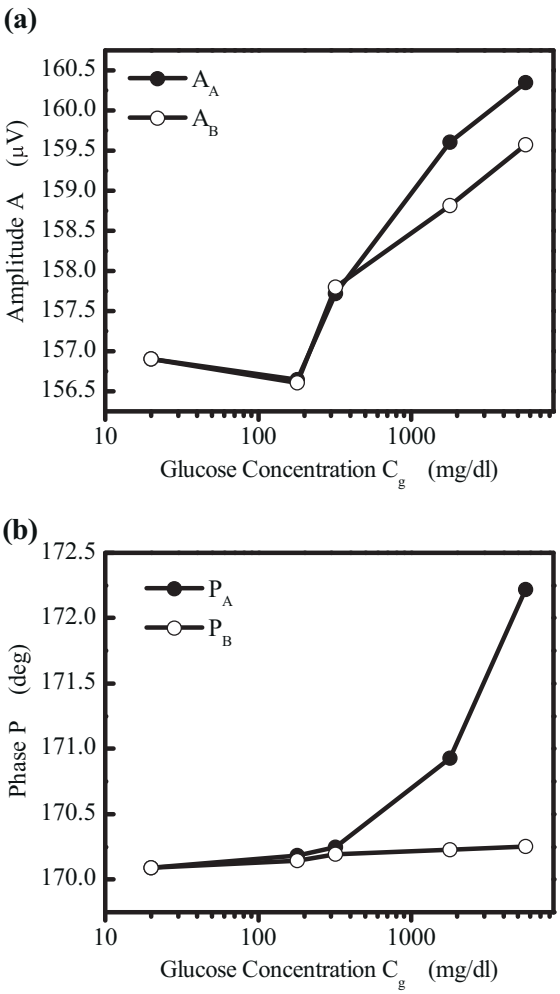

Figure 7 Single laser (laser *A* and laser *B*) PTR signals from serum-glucose solutions with glucose concentration from 20 mg/dl to 5600 mg/dl. (**a**) amplitude; (**b**) phase.

strated good reproducibility. Absorption spectroscopy [35] has shown a distinct glucose peak using wavelengths 8.38 μm and 9.65 μm. WM-DPTR exhibits clear superiority in NGM when compared with the aforementioned methods as shown in Table 1, especially in the hypoglycemic range which is clini-

Table 1 Comparison of MIR techniques.

Method	Sample	Predictive Standard Error (mg/dl)			
		$C_g < 75$ (mg/dl)		$C_g > 75$ (mg/dl)	
		amplitude	phase	amplitude	phase
WM-DPTR	blood serum	9.2	6.8	14.1	10.2
Pulsed Photoacoustic [31]	whole blood	–		linear data not available below 217 mg/dl	
Modulated Photoacoustic [29]	aqueous solution in epidermis	below detection limit (100 mg/dl)		not well resolved below 500 mg/dl	
Thermal Emission Spectroscopy [25]	tympanic membrane (in vivo)	27 (average)			
Absorption Spectroscopy [35]	blood serum	24.7 (average)			

cally most demanding of accuracy. Failure to detect hypoglycemia is the common error in the SMBG evaluation of state-of-the-art devices.

Comparisons of serum glucose measurements with the conventional single-ended PTR method were also performed. Measurements were made with only laser A or laser B as shown in Figure 7. The glucose concentration range spanned 20 mg/dl to 5600 mg/dl. Figure 7(a) shows that both amplitude A_A (from laser A) and A_B (from laser B) exhibit only small increases over this entire glucose concentration range, 2% in A_A and 1.6% in A_B. Over the physiological range (20 mg/dl to 320 mg/dl) there is a barely resolvable amplitude increase of ca. 0.6%. The phase P_A in Figure 7(b) exhibits a total increase of 2.13° over the full range, while P_B only increases by 0.16°. The phase change across the physiological range is 0.16° in P_A and 0.10° in P_B. The change of the signals from laser B is mainly due to the change in thermal properties of the sample (thermal diffusivity and thermal effusivity), while the change of signals from laser A is the result of changes in both optical and thermal properties of the sample. Comparison between Figures 5 and demonstrates the superior glucose sensitivity of WM-DPTR technology and its potential for clinical applications in the non-invasive measurement of blood glucose concentration.

4. Conclusions

We have reported the development of a WM-DPTR system for potential applications to non-invasive ISF glucose measurements. Glucose measurements in human serum, the best substitute for ISF, demonstrated that WM-DPTR is sensitive well above other optical, photoacoustic and photothermal noninvasive methodologies in the clinically relevant concentration range 20 mg/dl to 320 mg/dl. The achievement of optimal glucose sensitivity and measurement precision is the result of careful selection and tight control of two parameters: amplitude ratio R and phase shift dP of the two single baseline (pure serum) signals, which play the role of tuning system sensitivity by adjusting the intensity ratio and modulation phase shift of the two laser beams of the WM-DPTR system. The implementation of a motorized circular variable neutral density filter and phase-locked function generator into the system has resulted in high R resolution (0.003) and high dP resolution (0.05°). Optimal R-dP combinations have been found for linear and stable WM-DPTR response to serum glucose in the human physiological range with predictive standard error (<10.3 mg/dl) well below SMBG requirement. Thus WM-DPTR has been shown to be an excellent potential candidate for noninvasive glucose monitoring in a clinical setting. "As an important step to move toward in vivo non-invasive glucose detection, in-vitro measurements of human serum glucose diffused into human skin have been performed and will be reported next."

Acknowledgements The support of the NSERC-CIHR CHRP program, the Ontario Ministry of Research and Innovation (MRI) through the Premier's Inaugural Discovery Award to AM and the ORF program, and the Canada Foundation for Innovation (CFI) are gratefully acknowledged. We are grateful to Pranalytica Inc. for helpful discussions on, and partial support of, the QCL system.

Author biographies Please see Supporting Information online.

References

[1] D. B. Sacks, M. Arnold, G. L. Bakris, D. E. Bruns, A. R. Horvath, M. S. Kirkman, A. Lernmark, B. E. Metzger, and D. M. Nathan, Diab. Care **34**, 1419–1423 (2011).
[2] D. B. Sacks, M. Arnold, G. L. Bakris, D. E. Bruns, A. R. Horvath, M. S. Kirkman, A. Lernmark, B. E. Metzger, and D. M. Nathan, Diab. Care **34**, e61–e99 (2011).
[3] American Diabetes Association consumer guide – blood glucose meters, Diabetes Forecast (January 2012).
[4] American Diabetes Association consumer guide – continuous glucose monitors, Diabetes Forecast (January 2012).
[5] D. A. Gough, L. S. Kumosa, T. L. Routh, J. T. Lin, and J. Y. Lucisano, Sci. Transl. Med. **2**, 42–46 (2010).
[6] K. Billingsley, M. K. Balaconis, J. M. Dubach, N. Zhang, E. Lim, K. P. Francis, and H. A. Clark, Anal. Chem. **82**, 3707–3713 (2010).
[7] P. W. Barone, H. Yoon, R. Ortiz-Garcìa, J. Zhang, J. Ahn, J. Kim, and M. S. Strano, ACS Nano. **3**, 3869–3877 (2009).
[8] K. Lan, K. McAferty, P. Shah, E. Lieberman, D. R. Patel, C. B. Cook, and J. T. LaBelle, J Dia. Sci Technol. **5**, 1108–1115 (2011).
[9] Q. Yan, B. Peng, G. Su, B. E. Cohan, T. C. Major, and M. E. Meyerhoff, Anal. Chem. **83**, 8341–8346 (2011).
[10] R. McNichols and G. Coté, J. Biomed. Opt. **5**, 5–16 (2000).
[11] G. L. Coté, J. Nutr. **131**, 1596S–1604S (2001).
[12] A. Tura, A. Maran, and G. Pacini, Diab. Res. and Clin. Pract. **77**, 16–40 (2007).
[13] V. V. Tuchin (ed.), Handbook of Optical Sensing of Glucose in Biological Fluids and Tissues (CRC Press, Florida, 2008).
[14] C. E. Ferrante do Amaral and B. Wolf, Med. Eng. Phys. **30**, 541–549 (2008).
[15] S. K. Vashist, Anal. Chim. Acta., http://dx.doi.org/10.1016/j.aca.2012.03.043 (2012).

[16] N. A. Bazaev, Yu. P. Masloboev, and S. V. Selishchev, Bio. Eng. **45**, 229–233 (2012).
[17] C. Chou, C. Han, W. Kuo, Y. Huang, C. Feng, and J. Shyu, Appl. Opt. **37**, 3553–3557 (1998).
[18] B. H. Malik and G. L. Coté, J. Biomed. Opt. **15**, 017002 (2010).
[19] I. Barman, C. Kong, G. P. Singh, R. R. Dasari, and M. S. Feld, Anal. Chem. **82**, 6104–6114 (2010).
[20] J. L. Lambert, C. C. Pelletier, and M. Borchert, J. Biomed. Opt. **10**, 031110 (2005).
[21] R. Marbach, T. Koschinsky, F. A. Gries, and H. M. Heise, Appl. Spec. **47**, 875–881 (1993).
[22] K. Maruo, M. Tsurugi, M. Tamura, and Y. Ozaki, Appl. Spec. **57**, 1236–1244 (2003).
[23] C. Vrancic, A. Fomichova, N. Gretz, C. Herrmann, S. Neudecker, A. Pucci, and W. Petrich, Analyst **136**, 1192–1198 (2011).
[24] I. Gabriely, R. Wozniak, M. Mevorach, J. Kaplan, Y. Aharon, and H. Shamoon, Diab. Care **22**, 2026–2032 (1999).
[25] C. D. Malchoff, K. Shoukri, J. I. Landau, and J. M. Buchert, Diab. Care, **25**, 2268–2275 (2002).
[26] P. Zheng, C. E. Cramer, C. W. Barnes, J. R. Braig, and B. B. Sterling, Diab. Technol. Ther. **2**, 17–25 (2000).
[27] R. Ballerstadt, C. Evans, A. Gowda, and R. McNichols, Diab. Technol. Ther. **8**, 296–311 (2006).
[28] W. March, D. Lazzaro, and S. Rastogi, Diab. Technol. Ther. **8**, 312–317 (2006).
[29] J. Kottmann, J. M. Rey, J. Luginbühl, E. Reichmann, and M. W. Sigrist, Biomed. Opt. Exp. **3**, 667–680 (2012).
[30] G. Spanner and R. Niessner, Fresenius J. Anal. Chem. **354**, 327–328 (1996).
[31] G. B. Christison and H. A. McKenzie, Med. Biol. Eng. Comput. **31**, 284–290 (1993).
[32] C. J. Pouchert, The Aldrich Library of Infrared Spectra, 3 edn. (Aldrich Chemical Co., 1981).
[33] H. A. MacKenzie, H. S. Ashton, S. Spiers, Y. Shen, S. S. Freeborn, J. Hannigan, J. Lindberg, and P. Rae, Clin. Chem. **45**, 1587–1595 (1999).
[34] W. Martin, S. Mirov, and R. Venugopalan, J. Biomed. Opt. **7**, 613–617 (2002).
[35] W. Martin, S. Mirov, and R. Venugopalan, Appl. Spec. **59**, 881–884 (2005).
[36] X. Guo, A. Mandelis, A. Matvienko, K. Sivagurunathan, and B. Zinman, J. Phys.: Confer. Ser. **214**, 012025 (2010).
[37] X. Guo, A. Mandelis, and B. Zinman, Int. J. Thermophys. accepted (2012).
[38] A. Mandelis and X. Guo US patent pending No. 12/948,525 (2010).
[39] A. Mandelis and X. Guo, Phys. Rev. E **84**, 041917 (2011).
[40] K. J. Wientjes and A. J. Schoonen, Int. J. Artif. Organs **24**, 884–889 (2001).
[41] A. C. Guyton and J. E. Hall, Textbook of Medical Physiology (W.B. Saunders Co., Philadelphia, PA, 1996), pp. 971–983.
[42] B. P. Kovatchev, D. J. Cox, L. A. Gonder-Frederick, and W. L. Clarke, Diab. Care **27**, 1922–1928 (2004).
[43] ISO 15197, http://www.iso.org/iso/iso_catalogue/catalogue_tc/catalogue_detail.htm?csnum ber=26309 (2003).
[44] W. L. Clarke, D. Cox, L. A. Gonder-Frederick, W. Carter, and S. L. Pohl, Diab. Care **10**, 622–628 (1987).